STUDY AND PREDICTION OF THE FATIGUE LIFE OF AISI 1045 STEEL STRUCTURES UNDER ROTATIONAL BENDING STRESSES

Hichem YOUSFI[1], Mourad BRIOUA[2] , Rachid BENBOUTA[3]

Several difficulties and critical problems are facing the modern designers especially the unexpected damages. For such critical issues, the steel behavior's investigation presents a significant point to predict fatigue life through avoiding sudden damage. An experimental study has been conducted to evaluate the AISI 1045 steel fatigue behavior using three specimens' shapes: the first one is the conventional shape according to the ASTM E466-07 standard, the second one is performed in a notched shape, and the last specimen according to the pre-loading process. To complete the comparison among the three cases studied, a mandatory checking of the chemical compositions such as carbon content 0.45%, as well as the mechanical properties, have been investigated by preformed a tensile test in order to determine the maximum stress and the yield strength. The staircase method is employed to estimate and compare the endurance limit and its standard deviations for the three shapes. Moreover, and considered that the fatigue life expectancy of the AISI 1045 steel is a crucial step, the Stromeyer model has been proposed to predict the fatigue life which appears to be more effective, considering the average error for all cases compared to the experimental model.

Keywords: Fatigue life; AISI 1045 steel; tensile test; staircase method; endurance limit.

1. Introduction

Fatigue is the failure of a component under cyclic loading before it reaches its ultimate stress. Typically, the goal of fatigue testing is to determine the number of cycles required to fracture a specimen under a given set of loading conditions which allows engineers to estimate a structure's fatigue life [1-3]. Even though fatigue loading conditions can affect material behavior, the response of a structure may differ under extreme loading conditions [4].

Despite the practical importance of this phenomenon, several papers have been published that the effect of fatigue loading depends on the properties of unalloyed steels, especially the AISI 1045 steel [5-7]. One of the important procedures especially for components, based on the AISI 1045 steel, such as

[1] Asst. Prof. Dept. of Mechanical Engineering, University of BATNA 2, Algeria
[2] Prof., Dept. of Mechanical Engineering, University of BATNA 2, Algeria
[3] [3] Prof., Dept. of Mechanical Engineering, University of BATNA 2, Algeria, e-mail: r_benbouta@yahoo.fr

automobile engine, steering, and suspension parts is predicting the fatigue life of the part stressed above the endurance limit [1,8].

To analyze and predict the fatigue data, various technics and approaches can be used. These methods and technics were used to assess fatigue damage, predict fatigue life, and evaluate fatigue behaviors [9-11]. Guglielmino et al. [12] investigated the fatigue properties of AISI 1045, applying an infrared (IR) thermography method, as well as evaluate the energetic release during a tensile test even with a limited number of specimens. Experimental results show that this technic predict well the fatigue proprieties in short amount of time and a limited number of specimens. A new statistical-based analysis on the AISI 1045 steel have been conducted by Padzi et al. [13] to evaluate the fatigue life assessment at three different applied stresses during the cyclic testing procedure.

Using the Integrated Kurtosis-based Algorithm for Z-filter (I-kaz) approach, experimental results showed that the highest strain amplitude occur at the low frequency range, with the suggestion of the I-kaz approach to identify fatigue damage. Another experiment conducted on the influence of fatigue loading on the residual tensile properties of AISI 1045 steel. Two stages of research have been performed to estimate the elastic limit and the offset yield point values, results indicated that both parameters (initial and the pre-fatigued specimens) reach almost constant value after number of cycles equal to 25 % of the fatigue life. However, further increase in the number of cycles does not affect clearly the elastic limit and the offset yield point. Counterwise, decrease of both parameters value is observed at large number of pre-fatigue cycles corresponding to 75% of the fatigue life [14]. For aluminum alloys, similar analyses have been conducted with pre-strained specimens under high cycle fatigue loading conditions [15]. a very significant drop in the tensile force has been observed, while a second alloy was not affected by the initial fatigue. Moreover, and to address the notch effects in metal fatigue as well as damage modeling and fatigue life predictions, some researchers have been presented and developed theories and approaches to provide theoretical support for structural optimal design and integrity evaluation [16]. This work presents an experimental study of the influence of fatigue behavior (the endurance limit σ_D) on the characteristic of AISI 1045 steel which used frequently in various mechanical and electrical devices. Fatigue tests were performed according to the standard ASTM: E466-07. These tests involve three different specimens introduced as: the conventional, the notched and the pre-loaded (pre-fatigued) specimen.

2. Materials and methods

2.1 Chemical composition of the AISI 1045 steel

A comparison among different fatigues tests have been conducted, in which a mandatory checking process of the chemical compositions such as the carbon content 0.45%, and the mechanical characteristics through a tensile test have been done to determine the maximum stress σ_{max} and the elastic limit σ_e.

The chemical compositions of the AISI 1045 steel have been determined in the Seriana Industrial Achievement Establishment Physics Laboratory (ERIS) using an average mass spectrometer of two sparks on two steel pieces with a 15 mm in diameter for each piece.

2.2 Tensile test

Tensile tests were conducted on the AISI 1045 steel. These tests are the most used for the main mechanical characterizations of materials. They were performed on cylindrical specimens of fixing suitable shape. The specimens attached to the tensile test machine are subjected to uniaxial force.

The tests were carried out with a 500 Shimadzu UH500 universal test machine connected to a data control and acquisition computer. Also, a movement speed of 5 mm/min at an ambient temperature was applied to avoid the dynamic effects on material response.

The extensometer was fixed between the two location points defining the gauge length (G) in which the stress state is homogeneous. The geometry of the specimen is shown in Fig.1. This last one allows the identification of many standard sizes including the fracture stress, the maximum stress, the elasticity limits, the lengthening, etc., which necessarily needed in the structural calculations. The tensile test specimen has been prepared under the ASTM A370 standard [17].

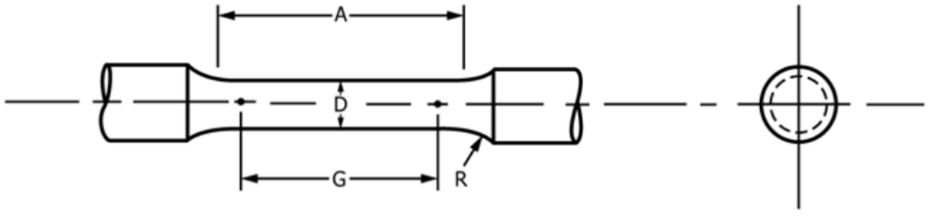

Fig. 1. The tensile test specimen geometry according to the standard (ASTM A370/ASME SA-370)

Different specimen's dimensions were used and realized according to the standards ASTM A370/ASME SA-370 [18], considering that this AISI 1045 steel was fabricated without any treatment or any specific way, as presented in Table 1.

Table 1

The specimen's dimensions

Dimensions in (mm)	Specimen N°1	Specimen N°2	Specimen N°3
G : Gauge length	50.0 ± 0.1	36.0 ± 0.1	24.0 ± 0.1
D : Diameter	12.5 ± 0.2	09.0 ± 0.1	06.0 ± 0.1
R : Radius of fillet	10	8	6
A : Length of reduced section	56	45	30

2.3 Rotational bending fatigue test

The experimental procedure has been divided into three important steps using Moore's test [19, 20] to investigate the fatigue behavior and the AISI 1045 steel characteristics:
Frst, the fatigue tests were carried out and followed by the analysis of the conventional specimens according the standard ASTM E466-07 (Fig. 2).
Next, the notched specimens were used to address the effect a notch in the middle of the pieces on the fatigue behavior [21, 22] as shown in Fig. 3.
Fnally, rotational bending tests of the pre-loaded specimens according the standard ASTM E466-07 were conducted to analyze in details the characteristics of the AISI 1045 steel.

For all the preformed tests the specimens were subjected to a rotary bending (4 points), with a stress ratio R equal to (R = –1) and purely alternating average stress (σ_m=0) [23, 24].

Moreover, the experiments were carried out on a technical specification test machine (Fig.4) (the maximum bending moment of 125 Nm, the rotational speed ranging from 2200 to 3000 rpm, the specimen's diameter of 15 mm, the maximum capacity of 10^9 cycles and the frequency of 50 Hz). The specimens were in a continuous rotational movement with a variable weight applied as presented in machine characteristic (Table 2).

Fig. 2. The conventional specimen shape and dimensions according to the ASTM E466-07 standard

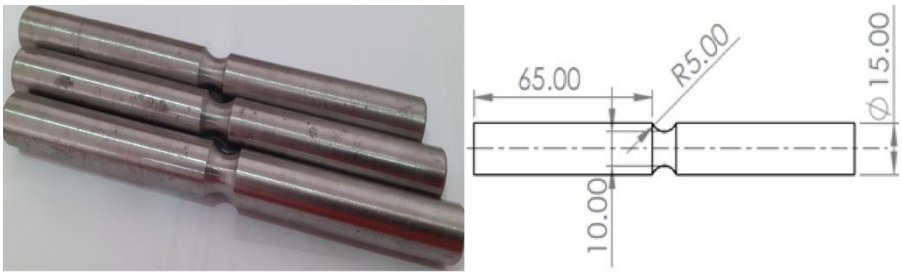

Fig. 3. The notched specimen shape and dimensions.

Fig. 4. Rotational bending test machine

Table 2

Rotational bending test machine description

N°	Description	N°	Description
1	Chassis	6	Mandrel
2	Control board	7	Plain bearing
3	Calculation computer	8	Specimen
4	Electrical motor	9	The applied weights
5	Drive shaft		

Staircase method was used to simplify the research for testing stress levels and the endurance limit determination. This method is most executable with a small number of attempts [25].

For the fatigue life prediction, the Stromeyer suggestion was used [26, 27] with an analytical estimation.

3. Results and discussion

3.1 Chemical compositions

To perform the experimental process using the AISI 1045 structural carbon steel, deferent chemical compositions was defined as shown in the Table 3.

Table 3

Chemical composition of the AISI 1045 steel, wt%

C%	Si%	Mn %	S %	Cr %	Ni %	Cu %	Iron%
0.45	0.28	0.633	0.02	0.158	0.08	0.171	98.2

3.2 Tensile test analysis

It was necessary to determine the mechanical properties of steel AISI 1045 in the order to carry the next experimental process, for this purpose, a lot of six specimens were tested. These significant experimental iterations are strongly needed as a strong point for an accurate description of the AISI 1045 steel characteristics.

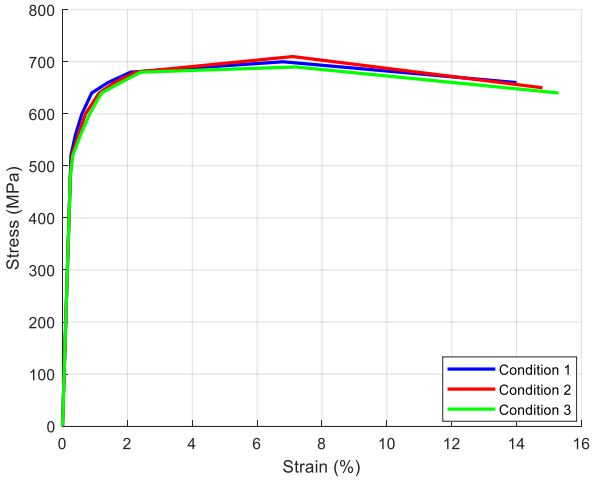

Fig. 5. Stress-Strain Diagram according to tensile test of AISI 1045 steel with three conditions

Fig. 5 shows the stress-strain diagram according to tensile test of AISI 1045 steel with different conditions, a very slight discrepancy among the three conditions. It seems to be that the different conditions especially the diameters (D_1 =12,5 mm, D_2 = 9 mm and D_3 = 6 mm) does not affect the stress-strain value. Even though the results obtain are foreseeable according with the performed testes and the specimens used, it is important to verify the mechanical proprieties of the AISI 1045 steel utilized before carry out the next experimental process.

The tensile test behavior of the selected steel is almost the same for all the three conditions. The conditions of the main mechanical characterizations well verified, while the AISI 1045 retains maximum strength for the second condition. The observations of elongations at fracture indicate a slight difference, but it does not significantly affect the properties of steel. The table 4 shows the optimal mechanical characteristics of the studied steel.

Table 4

Principal mechanical characteristics of AISI 1045 steel

Different conditions	The limit of Elasticity R_e(MPa)	Ultimate tensile strength R_m(MPa)	Tensile strength R_r(MPa)	elongation at fracture A%	Young Modulus E(MPa)
1st Condition	*520*	*700*	*660*	*14*	*200000*
2nd Condition	*510*	*710*	*650*	*14,8*	*200000*
3rd Condition	*500*	*690*	*640*	*15,3*	*200000*

3.3 Fatigue test behavior

3.3.1 Experimental models

3.3.1.1 The conventional shape vs. the notched shape

Fig.6 shows the experimental results as "curve (S-N)" for the conventional and the notched shape of the AISI 1045 steel specimens.

Results show a significant difference between the two shapes due to the heterogeneity of the material, surface defects, roughness "surface condition", especially the stress concentration factor.

In addition, it is observed that the endurance limit of the conventional shape is higher than that for the notched shape concerning that the rotating bending by approximately 10^7 cycles which is commonly used in literature [28]. Therefore, the fatigue strength (fatigue limit) by 10^7 cycles is estimated at (>315 MPa) for the conventional shape and (>300 MPa) for the notched shape.

It is also noticed that the fatigue life increases with the decrease in the stress's magnitude for both shapes.

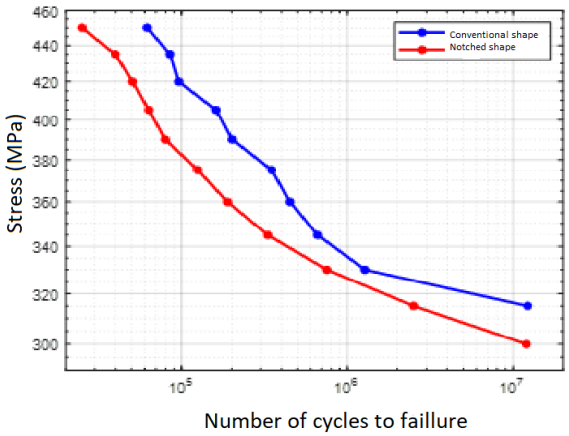

Fig. 6. The S-N comparison between the conventional and the notched shape

3.3.1.2 The conventional shape vs. the pre-loaded shape

Fig. 7 shows the experimental results as "curve (S-N)" for the conventional and the pre-loaded shape of the AISI 1045 steel specimens. It is observed that the difference seems to be noticeable in the limited endurance range from 10^4 up to 10^7cycles due to the impact of the pre-loaded effect on the test specimens. Counterwise, in the other domains especially in the olygocyclic domain (from 10^2 up to 10^4 cycles) and the unlimited endurance $N > 10^7$ a slight difference is observed. This result can be determined precisely with the staircase method.

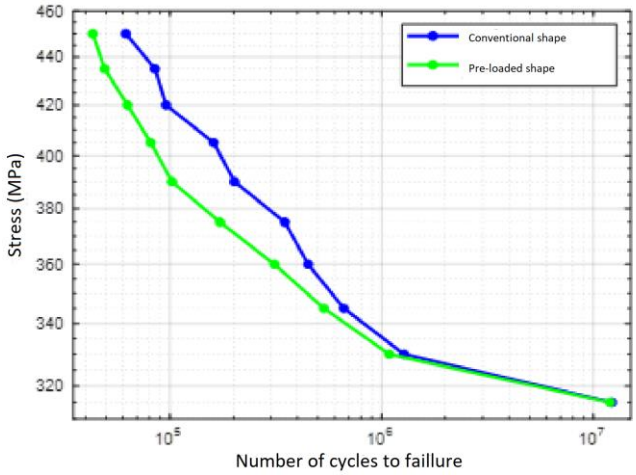

Fig. 7. The S-N comparison between the conventional and the pre-loaded shape.

3.3.2 Staircase procedure

The staircases are simulated from the whole test specimens (the conventional, the notched and the pre-loaded). The simulations were conducted simply by a comparison between the endurance limit of the randomly specimens and the stress amplitude applied at this loading level. If the applied stress is greater than the endurance limit, then there will be a failure of the specimens, and vice versa [29,30].

3.3.2.1 Conventional shape

Experimental tests of specimens for the conventional standard shape are carried out with alternating stress ranging from 295 to 340 MPa, as shown in Fig. 8. The endurance limit of this condition is found to be 319.375 ± 9.437 MPa.

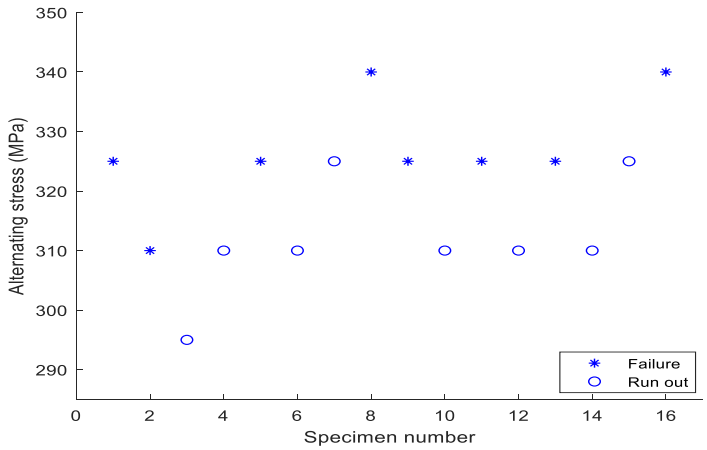

Fig. 8. Staircase fatigue test for the conventional shape

3.3.2.2 The notched shape

The staircase test of the specimens for the notched shape are performed with an alternating stress ranging from 285 to 345 MPa as shown in Fig. 9. The endurance limit for this condition is equal to 309.375 ± 17.79 MPa.

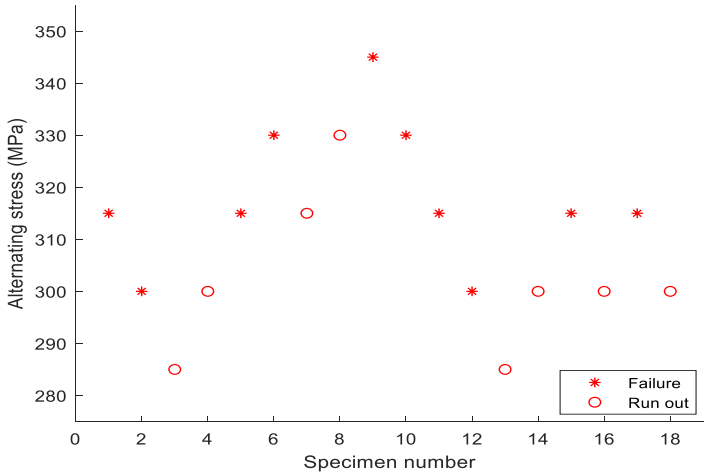

Fig. 9. Stair case fatigue test for the notched shape

3.3.2.3 The Pre-loaded shape

The staircase test of the pre-loaded shape with an alternative stress varied from 290 to 350 to MPa is shown in Fig. 10. The obtained endurance limit for this condition is 316.785 ± 26.49 MPa.

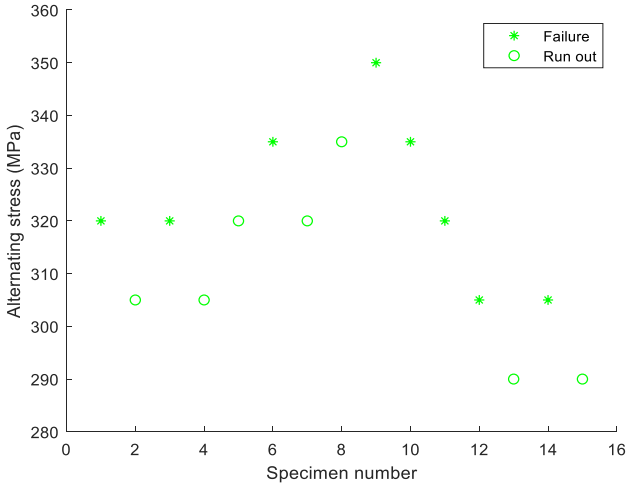

Fig.10. Stair case fatigue test for the pre-loaded shape.

Table 5

Test results for three type of specimens (MPa)

Shape	N	Median strength to rotary bending fatigue	Estimated standard deviation values ± Ds (MPa)
Standard Shape	16	319.375	± 9.437
Suggested Shape	18	309.375	± 17.79
Standard Pre-Loaded Shape Specimen	15	316.785	± 26.49

3.3.3 Analytical Models

In the literature reviews concerning the fatigue life, there are many expressions about fatigue models, in order to present the evolution of the stress as a function of the number of cycles during a cyclic loading. The best known properties are those suggested by Wöhler (1858) or Basquin (1910). Nevertheless, some authors suggest slightly different and more complex models [26]. The fatigue diagram (S-N curve) developed by Wöhler in 1858 has the longest history. Another estimate of fatigue analyzed in 1914 was Stromeyer suggestion [27] given by the following model:

$$Log\left(N_f\right) = a - b.Log\left(\sigma - \sigma_D\right) \tag{1}$$

where:

N_f: fatigue life in cycles (number of cycles to fatigue failure),

σ_D: stress amplitude,

a, b: parameters of the equation (constants of the regression model).

The Stromeyer's suggested model predict the fatigue life after a completed fatigue experiment. This approach helps to determine the cycle number and the endurance limits in which transform these loading conditions (N_f) and mechanical proprieties (σ_D) to a mathematical prediction expression.
By applying the Stromeyer's suggested model on the whole studied shapes, the following results for each shape are obtained:

Conventional Shape: $Log\left(N_f\right) = 7,9901 - 1,476\ Log(\sigma - 320)$

Notched shape: $Log\left(N_f\right) = 8,1096 - 1,6832\ Log\ (\sigma - 310)$

Pre-loaded shape: $Log\left(N_f\right) = 8,1895 - 1,6830\ Log(\sigma - 317)$

3.3.3.1 Errors analysis for the three shapes

Through the Stromyer's model comparisons have been done between (S-N) experimental curve and (S-N) analytical curve for the three shapes of the AISI 1045 steel used.

The conventional shape

Fig. 11 shows the experimental and the analytical results for the conventional shape; a slight difference of the curve results was observed in which the maximum error is in two points.

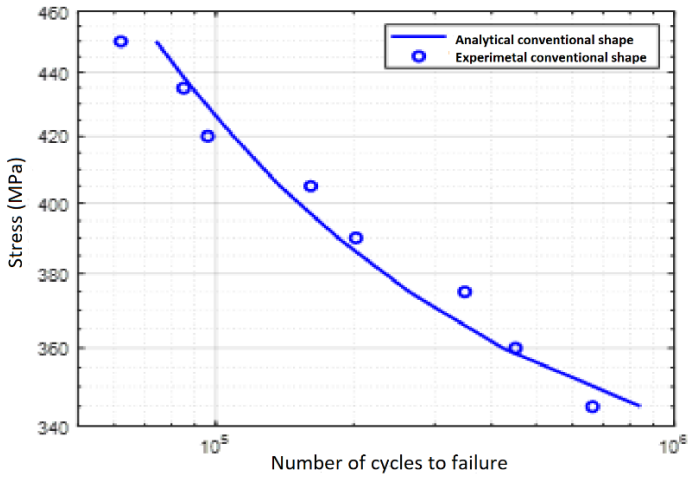

Fig. 11. Errors evolution on S-N curve for the conventional shape.

The notched shape

Fig. 12 shows the experimental and the analytical results for the notched shape; it is observed that there is a slight deference of the results curve in which the maximum error is in single point.

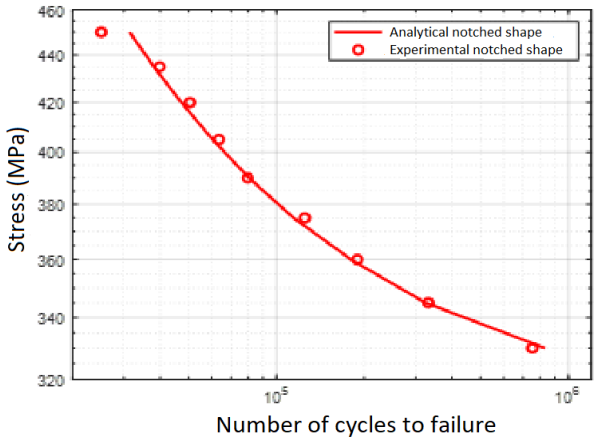

Fig. 12. Errors evolution on S-N curve for the notched shape.

The pre-loaded shape

Fig. 13 shows the experimental and the analytical results for the pre-loaded shape, also it seems that a slight difference noticed in which the maximum error is negligible.

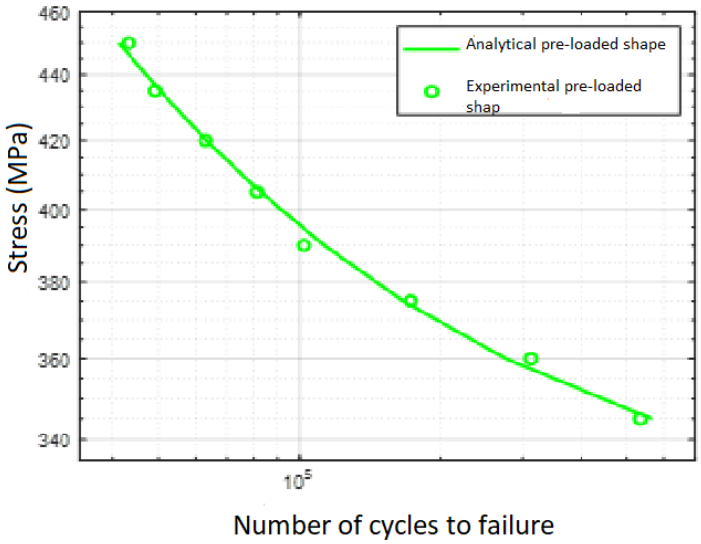

Fig. 13. Errors evolution on S-N curve for the pre-loaded shape.

Even though the graphical representation shows clearly the difference between the Stromeyer approach and the experimental results, it does not provide the real values for each type of the specimen shapes.

In order to obtain and clarify a well-verified relative error, Table 6 presents the relative errors for the experimental and the analytical model for the three specimen shapes.

Table 6

The relative error for the experimental and the analytical model

	Conventional shape			**Notched shape**			**Pre-loaded shape**		
stress	$LogN_{exp}$	$LogN_{ana}$	*E%*	$LogN_{exp}$	$LogN_{ana}$	*E%*	$LogN_{exp}$	$LogN_{ana}$	*E%*
450	4.7924	4.8699	1.62	4.3997	4.4972	2.22	4.6365	4.6149	-0.47
435	4.9294	4.9485	0.39	4.5999	4.58	-0.43	4.6920	4.7024	0.22
420	4.9823	5.0381	1.12	4.7033	4.6735	-0.63	4.8000	4.8019	0.04
405	5.2068	5.1423	-1.24	4.8021	4.7807	-0.45	4.9096	4.9169	0.15
390	5.3054	5.2667	-0.73	4.9009	4.9063	0.11	5.0099	5.0535	0.87
375	5.5428	5.4212	-2.19	5.0969	5.0581	-0.76	5.2370	5.2216	-0.29
360	5.6532	5.6254	-0.49	5.2767	5.2548	-0.42	5.4940	5.4403	-0.98
345	5.8215	5.9267	1.81	5.5202	5.5105	-0.18	5.7273	5.7538	0.46
330				5.8761	5.9197	0.74			

where:

$$E\% = \frac{logN_{ana} - LogN_{exp}}{LogN_{exp}} 100 \quad [31] \tag{2}$$

3.3.3.2 Analytic analysis among the conventional shape vs. the notched and the pre-loaded shape

For a better fatigue life prediction an analytic analysis through the Stromeyer model has been presented in a graphical representation among the three specimen shapes studied in this experimental paper.

Fig. 14 shows the analytical results of the conventional shape vs. the notched in term of fatigue testing (S-N) curve, it is noted that under the same stress and for all the calculated points, the fatigue life of the conventional shape is

higher than the fatigue life of the notched shape. The logarithmic direction lines (blue and red) are not in parallel path; a divergent observed for a higher stress value in the other hand, a convergent in S-N curve noticed for lower stress value.

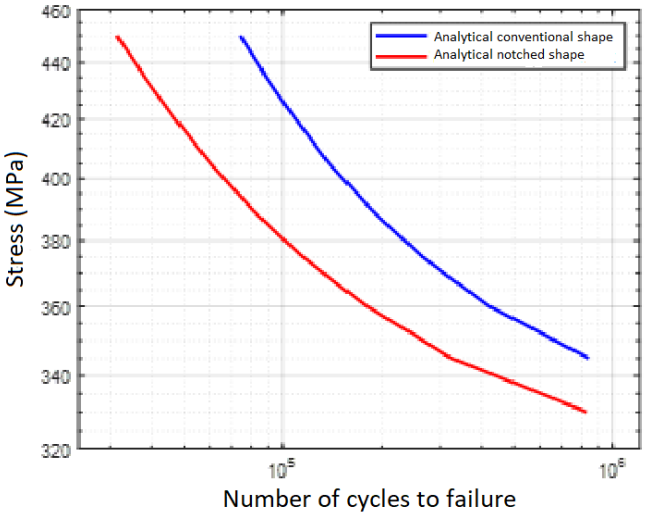

Fig. 14. The analytical (S-N) curve for the conventional shape vs. the notched shape model.

Fig. 15 shows the analytical results of the conventional shape vs. the pre-loaded in term of fatigue testing (S-N) curve; it is observed also that under the same stress value, the fatigue life of the conventional shape is the highest compared to the fatigue life of the pre-loaded one. It is clearly noticed that by reducing the stress value, the difference between the conventional and the pre-loaded model seems to be smaller.

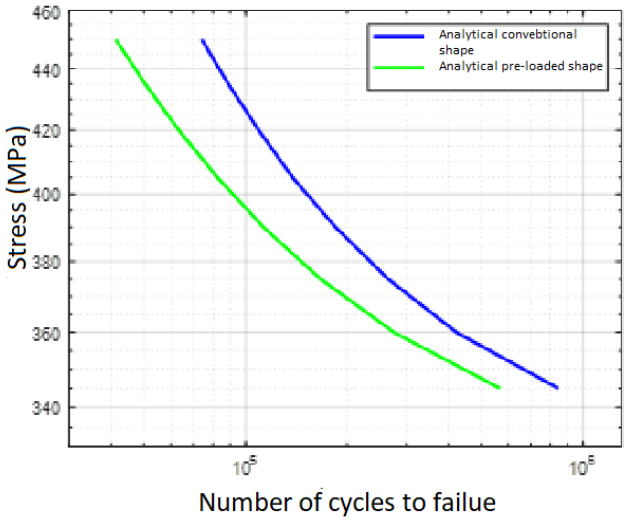

Fig. 15. The analytical (S-N) curve for the conventional shape vs. the pre-loaded shape model.

4. Conclusion

This experimental study shows how the fatigue behavior, through a tensile and rotational bending test, can be influenced by the geometrical and the loading conditions characteristics of three specimen shapes named: convectional, notched and pre-loaded based on AISI 1045 steel. For this reason, under the same loading conditions, a fair comparison between these three specimen shapes was made. Experimental and analytical model results conclude that:

- The needed of determine the mechanical characterization before any experiment process, for AISI 1045 steel identification and verification.
- The fatigue life can be influence by made a notch at the specimen middle which highly observed in olygocyclic and limited endurance domain, contrary in the unlimited endurance domain.
- The pre-loading process affect the fatigue life less than a notched specimen effect especially in the unlimited endurance domain when it seems to be similar to the conventional specimens.

In addition, the staircase method estimates and compares the endurance limit and its standard deviations for the whole cases studied: the conventional, the notched, and the pre-loaded specimen shapes. However, this work presents a proposed Stromeyer model for a better fatigue life prediction which appears to be more effective, considering the average error for all cases compared to the experimental model. This last one allows to verifies the well stress applied if the value of the cycle number known also defined the best model to avoid the over sizing.

R E F E R E N C E S

[1]. *L. Dietrich, J. Radziejewska, "*The fatigue damage development in a cast Al–Si–Cu alloy", Materials & Design", **vol. 32**, no 1, 2011, p. 322-329.

[2]. *Z. G. Hu, P. Zhu, J. Meng, "*Fatigue properties of transformation-induced plasticity and dual-phase steels for auto-body lightweight: Experiment, modeling and application", Materials & Design, **vol. 31**, no 6, 2010, p. 2884-2890.

[3]. *M. Ramesh, H.J. Leber, K. Janssens, M. Diener, R. Spolenak, "*Thermomechanical and isothermal fatigue behavior of 347 and 316L austenitic stainless tube and pipe steels", International Journal of Fatigue, **vol. 33**, no 5, 2011, p. 683-691.

[4]. *U. Sanchez-Santana, C. Rubio-Gonzalez, G. Mesmacque, A. Amrouche, X. Decoopman, "*Effect of fatigue damage induced by cyclic plasticity on the dynamic tensile behavior of materials", International Journal of Fatigue, **vol. 30**, no 10-11, 2008, p. 1708-1719.

[5]. *D.Y. Pimenov, A.T. Abbas, M.K. Gupta, I.N. Erdakov, M.S. Soliman, M.M. El Rayes, "*Investigations of surface quality and energy consumption associated with costs and material removal rate during face milling of AISI 1045 steel", The International Journal of Advanced Manufacturing Technology, **vol. 107**, no 7, 2020, p. 3511-3525.

[6]. *G. Contreras, C. Fajardo, J.A. Berríos, A. Pertuz, J. Chitty, H. Hintermann, "*Fatigue properties of an AISI 1045 steel coated with an electroless Ni-P deposit.", Thin Solid Films, **vol. 355**, 1999, p. 480-486.

[7]. *Y.L. Su, S.H. Yao, C.S. Wei, C.T. Wu, "*Influence of single-and multilayer TiN films on the axial tension and fatigue performance of AISI 1045 steel", Thin Solid Films, **vol. 338**, no 1-2, 1999, p. 177-184.

[8]. *G. Fourlaris, R. Ellwood, T.B. Jones, "*The reliability of test results from simple test samples in predicting the fatigue performance of automotive components", Materials & design, **vol. 28**, no 4, 2007, p. 1198-1210.

[9]. *U. P. Shine, E. M. S. Nair, "*Fatigue failure of structural steel–analysis using fracture mechanics",World Academy of Science, Engineering and Technology, **vol. 46**, 2008, p. 616-619.

[10]. *S. Q.Wang, J. H. Liu, D. L. Chen, "*Strain-controlled fatigue properties of dissimilar welded joints between Ti–6Al–4V and Ti17 alloys", Materials & Design, **vol. 49**, 2013, p. 716-727.

[11]. *C. Y. Seemikeri, P. K, Brahmankar, S. B. Mahagaonkar, "*Investigations on surface integrity of AISI 1045 using LPB tool", Tribology International, **vol. 41**, no 8, 2008, p. 724-734.

[12]. *E. Guglielmino, G. Risitano, D. Santonocito, "*A new approach to the analysis of fatigue parameters by thermal variations during tensile tests on steel", Procedia Structural Integrity, **vol. 24**, 2019, p. 651-657.

[13]. *M. M. Padzi, S. Abdullah, M. Z. Nuawi, "On* the need to decompose fatigue strain signals associated to fatigue life assessment of the AISI 1045 carbon steel", Materials & Design, **vol. 57**, 2014, p. 405-415.

[14]. *W. Moćko, "*The influence of stress-controlled tensile fatigue loading on the stress–strain characteristics of AISI 1045 steel", Materials & Design, **vol. 58**, 2014, p. 145-153..

[15]. *C. Froustey, J. L. Lataillade, "*Influence of the microstructure of aluminium alloys on their residual impact properties after a fatigue loading program", Materials Science and Engineering: A, **vol. 500**, no 1-2, 2009, p. 155-163.

[16]. *D. Liao, S.P. Zhu, J. Correia, "*Recent advances on notch effects in metal fatigue: A review. Fatigue & Fracture of Engineering Materials & Structures", **vol. 43**, no 4, 2020, p. 637-659.

[17]. *T. W. Kim, C. K. Jin, I. K. Jeong, S. S. Lim, J. C. Mun, C. G. Kang, J. D. Kim*, "Integral Steel Casting of Full Spade Rudder Trunk Carrier Housing for Supersized Container Vessels through Casting Process Engineering (Sekjin E&T) ", Metals, **vol. 5**, no. 2, 2015, p. 706-719.

[18]. Standard Test Methods for Tension Testing of Metallic Materials. E8/E8M − 16a.

[19]. *G. H. Majzoobi, F. Z. Jouneghani, E. Khademi*, "Experimental and numerical studies on the effect of deep rolling on bending fretting fatigue resistance of Al7075", The International Journal of Advanced Manufacturing Technology, **vol. 82**, no. 9-12, 2016, p. 2137-2148.

[20]. *F. Bozkurt, E. Schmidová*, "Fracture Toughness Evaluation of S355 Steel Using Circumferentially Notched Round Bars", Periodica Polytechnica Transportation Engineering, **vol. 47**, no. 2, 2019, p. 91-95.

[21]. *F. P. Yang, T. Chen, Y. C. Lu*, "The effects of carburization on the fatigue crack growth behaviors of local surface cracks in cylindrical bars", Journal of Materials Engineering and Performance, vol. 28, no. 6, 2019, p. 3423-3429.

[22]. *B. Castanié, V. Achard, C. Chirol*, "Effect of milled notches on the strength of open hole, filled holes, single and double lap shear CFRP tension coupons", Composite Structures, vol. 254, 2020, p. 112872.

[23]. *R. Fouchereau*, "Modélisation probabiliste des courbes SN", Doctoral Thesis, University Paris-Sud, France, 2014.

[24]. *Z. Jiang*, "Développement d'une machine de fatigue gigacyclique en torsion pour les matériaux métalliques à haute résistance", Doctoral Thesis, University Paris Nanterre, France, 2018.

[25]. *A. B. Venturini, T. C. Bohrer, P. E. Fontana, "*Step-stress vs. staircase fatigue tests to evaluate the effect of intaglio adjustment on the fatigue behavior of simplified lithium disilicate glass-ceramic restorations", Journal of the Mechanical Behavior of Biomedical Materials, **vol. 113**, 2021, p. 104091.

[26]. *A. Kurek, M. Kurek, T. Łagoda*, "Stress-life curve for high and low cycle fatigue", Journal of Theoretical and Applied Mechanics, **vol. 57**, no. 3, 2019, p. 677-684.

[27]. *C. E. Stromeyer*, "The determination of fatigue limits under alternating stress conditions", Proceedings of the Royal Society of London, Series A, 1914.

[28]. *H. Deng, W. Li, T. Sakai, Z. Sun*, "Very high cycle fatigue failure analysis and life prediction of Cr-Ni-W gear steel based on crack initiation and growth behaviors", Materials, **vol. 8**, no. 12, 2015, p. 8338-8354.

[29]. *V. Roué, S. Calloch, C. Doudard, A. Mattiello, Q. Pujol D'andrebo*, "Comparaison de différentes méthodes pour l'identification quantitative de la dispersion des essais de fatigue : simulation de procédures d'essais Staircase et comparaison avec la modélisation d'essais d'auto-échauffement", 24ème Congrès Français de Mécanique, Brest, 26 au 30 Août 2019.

[30]. *K. S. Lopes, W. F. Sales, E. S. Palma*, "Influence of machining parameters on fatigue endurance limit of AISI 4140 steel", Journal of the Brazilian Society of Mechanical Sciences and Engineering, **vol. 30**, no. 1, 2008, p. 77-83.

[31]. *M. Ravindran, M. Aswatha, N. Santhosh, G. Ravichandran, M. Madhusudhan*, "Effect of Heat Treatment on Fatigue Characteristics of En8 Steel". In IOP Conference Series: Materials Science and Engineering, **vol. 1013**, no. 1, 012009, IOP Publishing, 2021.